

Article

Study of Hydrogen-Induced Plastic Damage Response of 7085-T7651 High-Strength Aluminum Alloy

Xiao Yang ^{1,*}, Xianfeng Zhang ¹, Jieming Chen ¹, Zhenzhong Wang ¹, Xuefeng Li ¹, Xinyao Zhang ^{1,2} and Lingqing Gao ^{1,2}

¹ Luoyang Ship Material Research Institute, Luoyang 471023, China

² Henan Key Laboratory of Technology and Application Structural Materials for Ships and Marine Equipments, Luoyang 471023, China

* Correspondence: y19850419h@126.com; Tel.: +86-0379-67256734

Abstract: The hydrogen-induced plastic loss behavior of titanium alloys is often reported, but there are relatively few studies on high-strength aluminum alloys. In this article, the hydrogen-induced plastic damage behavior of 7085-T7651 high-strength aluminum alloy was investigated using a tensile specimen with pre-charging hydrogen, and the microstructure was characterized by transmission electron microscopy, scanning electron microscopy and time-of-flight secondary ion mass spectrometry. The results showed that 7085-T7651 high-strength aluminum alloy material has certain hydrogen embrittlement sensitivities, and with the increase of hydrogen-charging time, the hydrogen content and sensitivity of the material increases significantly. For the first time, the theoretical analysis and intuitive quantitative characterization of the hydrogen-induced plastic loss behavior mechanism on 7085-T7651 high-strength aluminum alloy is stated as the formation of Mg and H segregation formed at the crystal boundary, which will result in the weakening of the crystal boundary.

Keywords: 7085-T7651 high-strength aluminum alloy; hydrogen; plastic damage; characterization; brittleness



Citation: Yang, X.; Zhang, X.; Chen, J.; Wang, Z.; Li, X.; Zhang, X.; Gao, L. Study of Hydrogen-Induced Plastic Damage Response of 7085-T7651 High-Strength Aluminum Alloy. *Metals* **2023**, *13*, 40. <https://doi.org/10.3390/met13010040>

Academic Editor: Francesco Iacoviello

Received: 31 October 2022
Revised: 24 November 2022
Accepted: 4 December 2022
Published: 23 December 2022



Copyright: © 2022 by the authors. Licensee MDPI, Basel, Switzerland. This article is an open access article distributed under the terms and conditions of the Creative Commons Attribution (CC BY) license (<https://creativecommons.org/licenses/by/4.0/>).

1. Introduction

The 7xxx high-strength aluminum alloy belongs to the ultra-high-strength aluminum alloy Al-Zn-Mg-Cu series. This alloy is a newly developed high-performance aluminum alloy with excellent comprehensive properties such as high strength, high hardenability and high damage tolerance [1–3]. It has been widely used in aerospace, shipbuilding and other fields [4–6]. Generally speaking, there are two main failure behaviors of high-strength aluminum alloys. One is stress-corrosion cracking (SCC) caused by corrosion [7] and stress, and the other is environment-induced hydrogen and hydrogen-induced damage. There are many studies on stress-corrosion cracking of high-strength aluminum alloys [8–12]. However, there are relatively few studies on environmentally induced hydrogen and hydrogen-induced damage to high-strength aluminum alloys. Swapnar et al. [13] showed that, at intermediate strain rates, the film interfered and reduced hydrogen entry at intermediate strain rates, while hydrogen embrittlement was significant at the slowest strain rates. Komazaki [14] revealed that hydrogen was absorbed into the alloy by flux treatment and hydrogen content tended to increase with increasing exposure time. However, hydrogen is difficult to detect, and has strong diffusivity in materials. At present, most elemental analysis equipment cannot characterize and quantitatively analyze hydrogen intuitively, and most research on hydrogen interaction mechanisms and damage behavior is inferences, and there is no intuitive evidence. In particular, hydrogen-induced plastic damage behavior of 7085-T7651 high-strength aluminum alloy is still unclear.

In this paper, the influence of hydrogen on the plasticity of materials was studied by pre-filling hydrogen in tensile specimens for different time periods, and the depth of hydrogen action was analyzed using a hardness test. Meanwhile, time-of-flight secondary ion mass spectrometry (TOF-SIMS) was used to observe the hydrogen distribution visually and quantitatively near and far from the fissure.

2. Experimental Procedure

2.1. Materials

The studied 7085-T7651 high-strength aluminum alloy has high strength, good resistance to exfoliation corrosion and stress-corrosion resistance. The aluminum alloy ingot was homogenized at 450~480 °C for 24 h, and then free forging was carried out. Three-level enhanced solid solution was used to heat treatment. The measured composition of the 7085-T7651 high-strength aluminum alloy was Al-7.3Zn-1.5Mg-1.5Cu-0.10Zr.

Samples were cut from the 7085-T7651 high-strength aluminum alloy ingot and polished using silicon carbide grinding papers from 180 to 2000 grit. Microstructures were analyzed using an optical microscope (OM, equipment model: Leica DMI5000M, Leica, Wetzlar, Germany) and transmission electron microscope (TEM: equipment model: JEM-2100, JEOL, Tokyo Japan). The metallographic structure of the 7085-T7651 high-strength aluminum alloy was α (Al) + dispersed phase + compound phase. The grain size of the 7085-T7651 high-strength aluminum alloy was relatively uniform with a grade of 5.0. The compound phase was MgZn_2 , which precipitated along the grain boundary, as shown in Figure 1.

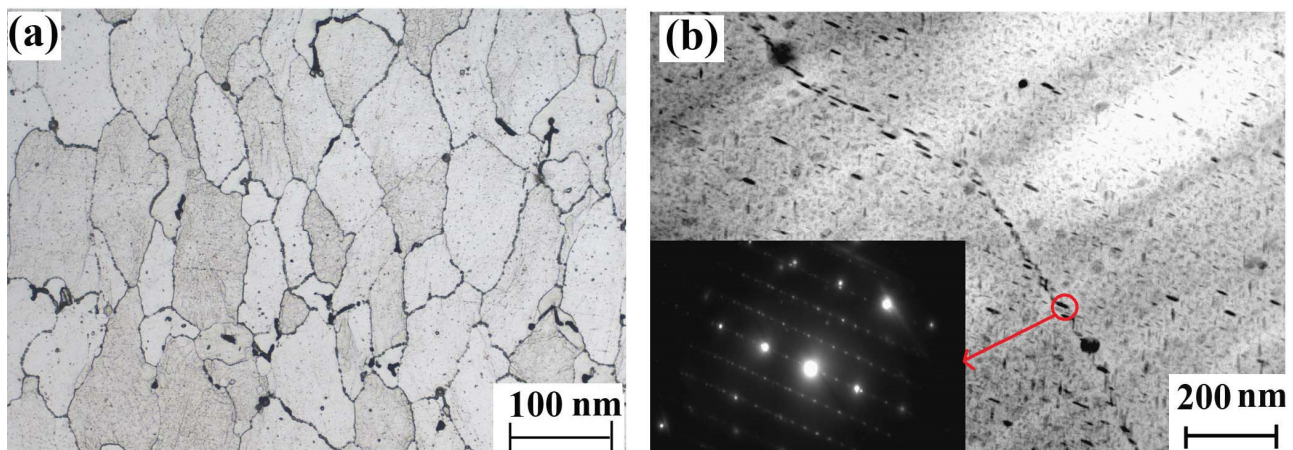


Figure 1. Microstructure of the 7085-T7651 high-strength aluminum alloy: (a) OM morphology and (b) TEM morphology and diffraction spots of the precipitated phase.

2.2. Pre-Charge Hydrogen

The selected electrochemical cathode hydrogen permeation method was pre-charge hydrogen. The sample and a carbon rod were used as the cathode and anode, respectively. Before pre-charge hydrogen, a calibrated DC-regulated power supply was selected. The electrolyte component was an aqueous ammonium sulfate solution. During hydrogen permeation, the current density was controlled at 2 mA/cm², the solution concentration was 5%, and the hydrogen-charging time was 5 days, 10 days, and 20 days, respectively. To avoid long-term storage of hydrogen-charged samples in the atmosphere, all samples were stretched within 2 h.

The hydrogen content was measured by German EltraONH-2000 analyzer and the GB/T 223.82-2018 standard [15]. The crucible was a heating body, and impurities were removed by degassing at high temperature. The sample was first removed from the surface hydrogen in a carrier gas (argon), and then melted. The hydrogen was detected by a thermal conductivity detector for detection. The penetration depth of hydrogen in the

7085-T7651 high-strength aluminum alloy was measured by microhardness tester (VH3300, Wilson, Chicago, IL, USA) according to the ASTM 384 standard [16].

TOF-SIMS technology performed intuitive and quantitative analysis of hydrogen in materials [17,18]. The TOF-SIMS equipment is produced by Czech Tesken.

2.3. Plastic Loss Behavior

Plastic loss behavior was comprehensively reflected by the elongation and fracture morphology of the tensile specimen. The selected sample size is shown in Figure 2 and the test method reference was the standard ASTM E8 [19]. The fracture of the tensile specimen was observed by FEI QUANTA650 Field Emission Scanning Electron Microscopy.

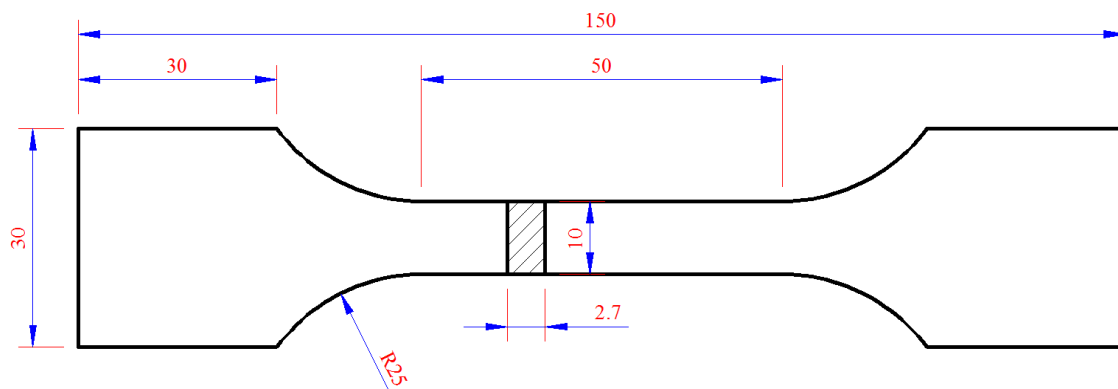


Figure 2. The dimensions of the tensile specimens (mm).

Multiple tensile 7085-T7651 high-strength aluminum alloy samples were processed on the same ingot. The surface of each sample was polished to reduce the surface roughness and keep the roughness as consistent as possible. Among them, the uncharged samples were numbered #1, and the samples charged with hydrogen for 5 days, 10 days, and 20 days were numbered #2, #3 and #4, respectively.

3. Results and Discussion

3.1. Hydrogen-Induced Plastic Damage

The properties of all samples after stretching are shown in Table 1. The elongation rate of sample #1 is about 4.9%; the elongation rate of #2, #3 and #4 is about 2.9%, 1.8% and 1.0%, respectively. As shown in Table 1, the elongation rate of all hydrogen-charged samples is significantly reduced. This suggests that the sample charged with hydrogen could cause obvious damage to the plasticity of the 7085-T7651 high-strength aluminum alloy. Meanwhile, with the increase of hydrogen-charging time, the strength also increases slightly.

Table 1. The properties and hydrogen content of 7085-T7651 high-strength aluminum alloy in different states.

Sample No.	Hydrogen Content (ppm)	Properties	
		Rm (MPa)	A (%)
1	0.8, 1.3, 1.1 (σ : 0.25)	444, 448, 443 (σ : 2.65)	5.2, 5.0, 4.5 (σ : 0.36)
2	2.8, 3.1, 3.3 (σ : 0.25)	472, 465, 470 (σ : 3.61)	2.6, 2.9, 3.2 (σ : 0.30)
3	5.4, 5.1, 5.2 (σ : 0.15)	475, 478, 478 (σ : 1.73)	2.1, 1.5, 1.7 (σ : 0.31)
4	5.6, 6.1, 6.0 (σ : 0.26)	488, 472, 477 (σ : 8.19)	1.0, 0.8, 1.2 (σ : 0.20)

To study the hydrogen content of the tensile sample under different hydrogen-charging time, a sample with 50 mm \times 3 mm \times 3 mm was also charged under the same hydrogen-charging conditions. Three parallel samples were selected for the test samples. The average hydrogen content in a blank sample was only 1.1 ppm, while the samples after

5 days, 10 days and 20 days hydrogen charging were about 3.1 ppm, 5.2 ppm and 5.9 ppm, respectively. Therefore, the hydrogen content in the 7085-T7651 high-strength aluminum alloy samples increases with the hydrogen-charging time.

From the test results, the 7085-T7651 high-strength aluminum alloy has similar characteristics to steel and titanium alloys. It has a certain solubility for hydrogen, and with the extension of hydrogen-charging time, the hydrogen content in the material increases. Meanwhile, damage behavior is also the same as other metals, i.e., there is obvious hydrogen-induced plastic damage behavior in high-strength aluminum alloys.

3.2. Section Analysis

Figure 3 shows the morphology of different areas on the tensile section of the blank sample without hydrogen charging. Many dimples can be observed, while no obvious brittle fracture features can be found on the entire section.

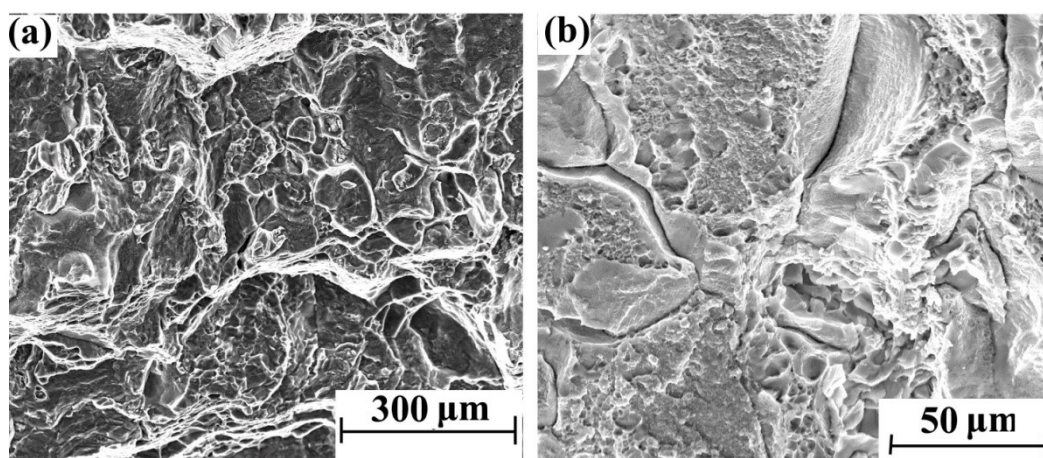


Figure 3. Tensile fracture morphology of blank sample without hydrogen charging: (a) 500 \times and (b) 2000 \times .

With the increase of hydrogen content, the fracture brittleness is gradually enhanced. The tensile fracture morphology with different regions after 5 days of hydrogen charging is shown in Figure 4a,b. There were obvious intergranular fracture characteristics in some areas of the cross-section, but the main morphological characteristics are still parabolic dimples. The tensile fracture morphology with different regions after 10 days of hydrogen charging is shown in Figure 5a,b. Compared with the sample with 5 days hydrogen charging, the intergranular fracture area is significantly increased. Furthermore, the parabolic dimples of the crystal plane are reduced, and the dimple openings are smooth. Therefore, the shape of the dimple is slightly inconspicuous. The tensile fracture morphology with different regions after 20 days of hydrogen charging is shown in Figure 6a,b, where there are more intergranular fracture areas on the entire cross-section. After the crystal plane enlargement, no obvious parabolic dimple morphology is observed, and a brittle ridge fracture is mainly observed.

3.3. Hardness Analysis

Watson et al. [20] researched the effects of cathodically charged hydrogen on the mechanical properties. The results showed that hydrogen charging could reduce the ductility, increase the tensile strength in tensile tests and form a severely hardened surface region due to increased dislocation density. The hardness surface region quickly saturated, and further charging increased the depth of this region. Hence, the depth of hydrogen infiltration can be determined according to the microhardness change in the material from surface to core. To further verify the influence of hydrogen on the alloy, a hardness analysis on the samples charged with hydrogen for 20 days was conducted. The American Wilson VH3300 microhardness meter used in the hardness test and parameter setting had a test

force of 10 g, hardness point intervals of 10 microns, and the hardness test was on the straight line from surface to core. The sudden change point on the hardness change curve is taken to be the hydrogen infiltration depth.

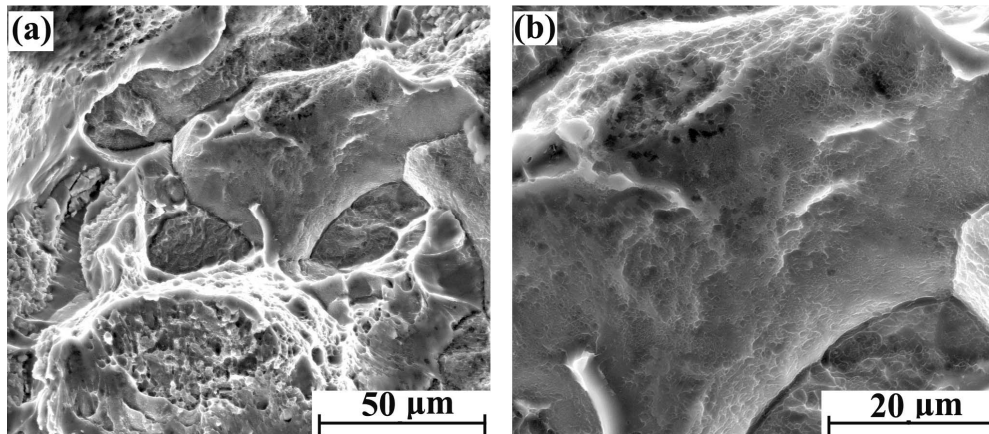


Figure 4. Tensile fracture morphology of hydrogen-charged sample for 5 days: (a) 2000× and (b) 5000×.

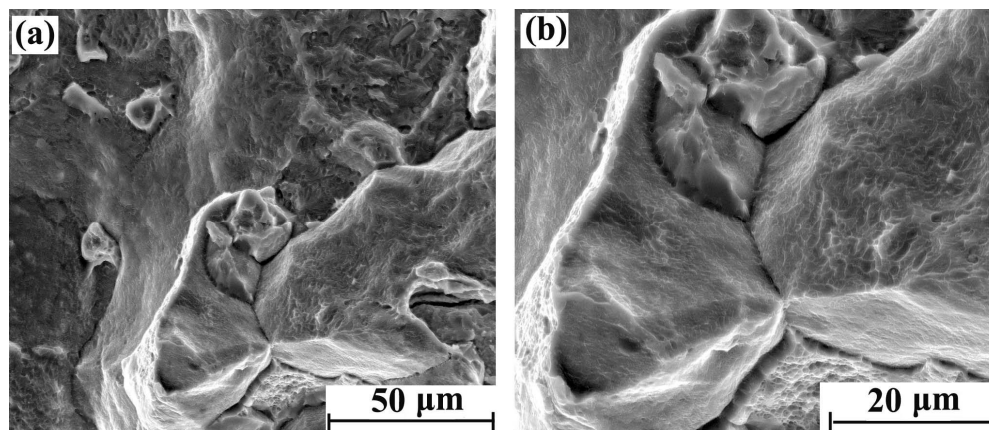


Figure 5. Tensile fracture morphology of hydrogen-charged sample for 10 days: (a) 2000× and (b) 4000×.

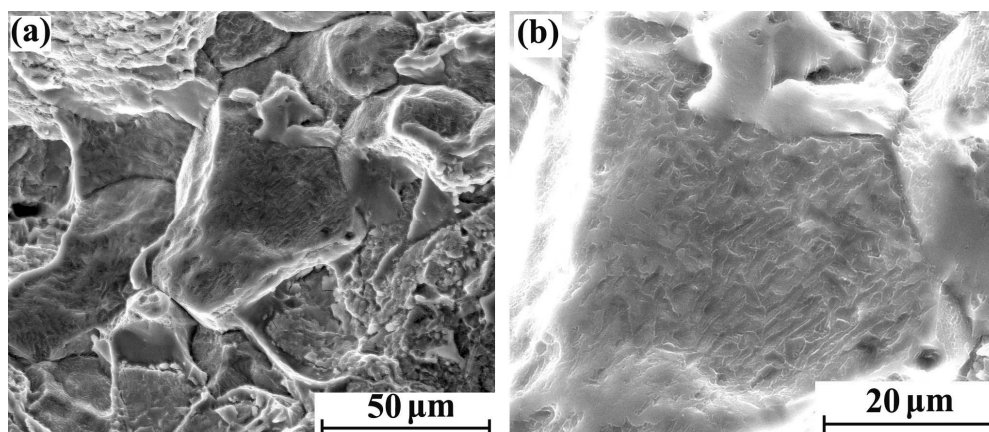


Figure 6. Tensile fracture morphology of hydrogen-charged sample for 20 days: (a) 2000× and (b) 5000×.

The microhardness gradient of hydrogen-filled samples was analyzed from surface to core. The result is shown in Figure 7. The microhardness of the hydrogen-charged sample changed significantly from the surface to the core, and the hardness turning point was at about 210 μm from the surface. Therefore, charging hydrogen in a 7085-T7651 high-strength aluminum alloy at a current density of $2 \text{ mA}/\text{cm}^2$ for 20 days could make the penetration depth of hydrogen approximately 210 μm , and the surface hardness of the hydrogen-permeable area significantly increased.

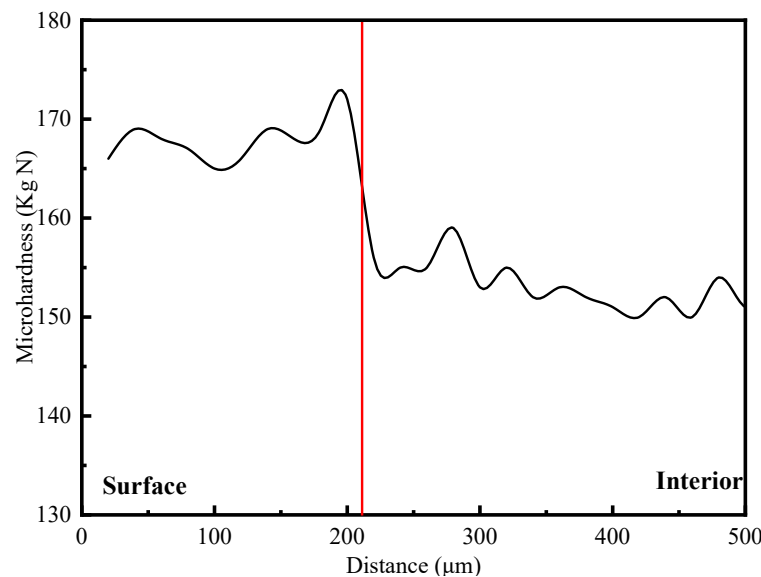


Figure 7. The hardness change in the hydrogen-charged sample.

For metals, hydrogen permeation can improve the strength of materials. The hardness test results of hydrogen-filled materials also prove that the high-strength aluminum alloy after hydrogen filling has a strengthening effect.

3.4. Hydrogen Analysis

The intuitive and quantitative analyses of hydrogen were performed on tensile samples after pre-charge for 20 days by TOF-SIMS. The peak area was obtained by pseudo-Voigt fitting of the hydrogen peak positions in TOF-SIMS, which is proportional to the hydrogen content. Therefore, we can obtain the relative hydrogen content of different regions of the same sample under the same test conditions by calculating the hydrogen peak area. The test results of hydrogen near the fracture and far from the fracture were shown in Figure 8. The values near the fracture and far from the fracture are 0.000019 and 0.000003, respectively. It can be deduced that the content of hydrogen near the fracture is higher than that far from the fracture.

3.5. Mechanism Analysis

Through test analysis, it can be found that the strength and plasticity of the material were obviously reduced when hydrogen was introduced into materials. In addition, with the increase of hydrogen content, the plasticity of the material decreased more obviously. Generally speaking, the index of hydrogen embrittlement susceptibility (HEI) was calculated according to the following formula [21]:

$$\text{HEI} = \frac{\varphi_F - \varphi_C}{\varphi_F} \quad (1)$$

where φ_F and φ_C represent the elongation rate of hydrogen-free specimen and hydrogen-charged specimen, respectively.

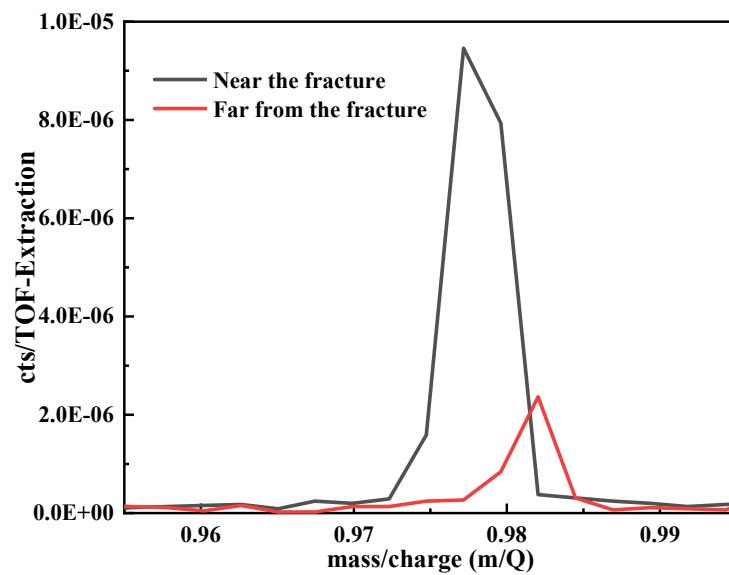


Figure 8. The integrated area of hydrogen peak.

The calculation results show that the HEI of the samples charged with hydrogen for 5 days, 10 days, and 20 days was about 40.82%, 63.27% and 79.59%, respectively. It concluded that 7085-T7651 high-strength aluminum alloy material has a certain hydrogen embrittlement sensitivity, and with the increase of hydrogen-charging time, the hydrogen content of the material increases significantly, and the hydrogen embrittlement sensitivity also increases.

The tensile fracture shows that the samples without hydrogen filling have mainly dimple fracturing, but, after hydrogen charging, they are mainly characterized by intergranular fracture. Moreover, with the prolongation of hydrogen-charging time, the intergranular fracture characteristics of the material become more obvious, and the dimple fracture characteristics gradually disappear. This morphology change, from dimple to intergranular, is a typical characteristic caused by hydrogen in materials [22,23]. In addition, the fracture characteristics along the grain also prove that hydrogen acts mainly at the grain boundary of the material.

Since the aluminum alloy has a face-centered cubic structure and the solubility of hydrogen in aluminum is extremely small, it is considered that hydrogen embrittlement does not exist in the aluminum alloy for a long period of time. However, with the deepening of research, it can be found that hydrogen embrittlement is also one of the common failure modes in high-strength aluminum alloys. Meanwhile, Song et al. [10] reported that hydrogen-induced cracking behavior exists in high-strength aluminum alloys and proved that Mg and H segregation formed at the grain boundary, which leads to the grain boundary weakening and initiates intergranular cracking.

4. Conclusions

- (1) 7085-T7651 high-strength aluminum alloy has a certain hydrogen-absorption capacity, which might cause hydrogen-induced plastic damage behavior in the service process.
- (2) The hydrogen-induced plastic damage behavior of the 7085-T7651 high-strength aluminum alloy is mainly characterized by intergranular fracture, which is due to the formation of Mg and H segregation formed at grain boundaries, leading to the embrittlement of the material.
- (3) Hydrogen-induced plastic damage and hydrogen-induced cracking behavior of 7085-T7651 high-strength aluminum alloy can be intuitively and quantitatively characterized using the TOF-SIMS method.

- (4) To further understand the effect of hydrogen on high-strength aluminum alloy, we will continue to research the characterization technology of micro–nano structures and the distribution of hydrogen at the crystal boundary.

Author Contributions: X.Y. conceived and designed the experiments; X.Y. and X.Z. (Xianfeng Zhang) performed the experiments; X.Y., X.Z. (Xianfeng Zhang), Z.W. and X.L. analyzed the data; J.C., X.Z. (Xinyao Zhang) and L.G. contributed reagents/materials/analysis tools; X.Y. wrote the paper. All authors have read and agreed to the published version of the manuscript.

Funding: This research received no external funding.

Institutional Review Board Statement: Not applicable.

Informed Consent Statement: Not applicable.

Data Availability Statement: The data presented in this study are available on request from the corresponding author. The data are not publicly available due to privacy.

Conflicts of Interest: The authors declare no conflict of interest.

References

1. Williams, J.C.; Starke, E.A., Jr. Progress in structural materials for aerospace systems. *Acta Mater.* **2003**, *51*, 5775–5799. [[CrossRef](#)]
2. Staley, J.T.; Liu, J. Aluminum alloys for aero structures. *Adv. Mater. Process.* **1997**, *152*, 17–20.
3. Heinz, A.; Haszler, A.; Keidel, C.; Moldenhauer, S.; Benedictus, R.; Miller, W.S. Recent development in aluminium alloys for aerospace applications. *Mater. Sci. Eng. A* **2000**, *280*, 102–107. [[CrossRef](#)]
4. Prabhu, T. An overview of high-performance aircraft structural Al alloy-AA7085. *Acta Metall. Sin. (Engl. Lett.)* **2015**, *28*, 909–921. [[CrossRef](#)]
5. Zhou, B.; Liu, B.; Zhang, S. The advancement of 7xxx series aluminum alloys for aircraft structures: A review. *Metals* **2021**, *11*, 718. [[CrossRef](#)]
6. Dursun, T.; Soutis, C. Recent developments in advanced aircraft aluminium alloys. *Mater. Des.* **2014**, *56*, 862–871. [[CrossRef](#)]
7. Kairy, S.K.; Turk, S.; Birbilis, N.; Shekhter, A. The role of microstructure and microchemistry on intergranular corrosion of aluminium alloy AA7085-T7452. *Corros. Sci.* **2018**, *143*, 414–427. [[CrossRef](#)]
8. Chen, S.Y.; Chen, K.H.; Dong, P.X.; Ye, S.P.; Huang, L.P. Effect of heat treatment on stress corrosion cracking, fracture toughness and strength of 7085 aluminum alloy. *Trans. Nonferrous Met. Soc. China* **2014**, *24*, 2320–2325. [[CrossRef](#)]
9. El-Amoush, A.S. Investigation of corrosion behavior of hydrogenated 7075-T6 aluminum alloy. *J. Alloys Compd.* **2007**, *443*, 171–177. [[CrossRef](#)]
10. Song, R.G.; Dietzel, W.; Zhang, B.J.; Liu, W.J.; Tseng, M.K.; Atrens, A. Stress corrosion cracking and hydrogen embrittlement of an Al-Zn-Mg-Cu alloy. *Acta Mater.* **2004**, *52*, 4727–4743. [[CrossRef](#)]
11. Rao, A.U.; Vasu, V.; Govindaraju, M.; Srinadh, K.S. Stress corrosion cracking behavior of 7xxx aluminum alloys: A literature review. *Trans. Nonferrous Met. Soc. China* **2016**, *26*, 1447–1471. [[CrossRef](#)]
12. Chen, S.Y.; Chen, K.H.; Peng, G.S.; Liang, X.; Chen, X.H. Effect of quenching rate on microstructure and stress corrosion cracking of 7085 aluminum alloy. *Trans. Nonferr. Metal. Soc.* **2012**, *22*, 47–52. [[CrossRef](#)]
13. Dey, S.; Chattoraj, I. Interaction of strain rate and hydrogen input on the embrittlement of 7075 T6 Aluminum alloy. *Mater. Sci. Eng. A* **2016**, *661*, 168–178. [[CrossRef](#)]
14. Komazaki, S.I.; Kobayashi, K.; Nakayama, T.; Kohno, Y. Evaluation of Susceptibility to Hydrogen Embrittlement of 7075 Aluminum Alloy by Hydrogen Addition Using Flax-Treatment Method. *Mater. Trans.* **2006**, *47*, 1994–1998. [[CrossRef](#)]
15. GB/T 223.82-2007; Steel and Iron—Determination of Hydrogen Content—Inert Gas Impulse Fusion Heat Conductivity Method. Chinese Technical Standard: Beijing, China, 2007.
16. E384-09; Standard Test Method for Microindentation Hardness of Materials. ASTM Standards: West Conshohocken, PA, USA, 2009.
17. Yang, X.; Luo, X.; Zhang, X.; Chen, J.; Gao, L. Characterization of hydrogen in a high strength aluminum alloy. *Mater. Test.* **2020**, *62*, 962–964. [[CrossRef](#)]
18. Hamada, S.; Ohnishi, K.; Nishikawa, H.A.; Oda, Y.; Noguchi, H. SIMS analysis of low content hydrogen in commercially pure titanium. *J. Mater. Sci.* **2009**, *44*, 5692–5696. [[CrossRef](#)]
19. E8/E8M-16a; Standard Test Methods for Tension Testing of Metallic Materials. ASTM Standards: West Conshohocken, PA, USA, 2016.
20. Watson, J.W.; Meshii, M.; Shen, Y.Z. Effect of cathodic charging on the mechanical properties of aluminum. *Metall. Trans. A* **1988**, *19*, 2299–2304. [[CrossRef](#)]
21. Shen, S.; Li, X.; Zhang, P.; Nan, Y.; Yang, G.; Song, X. Effect of solution-treated temperature on hydrogen embrittlement of 17-4 PH stainless steel. *Mater. Sci. Eng. A* **2017**, *703*, 413–421. [[CrossRef](#)]

22. Bechtle, S.; Kumar, M.; Somerday, B.P.; Launey, M.E.; Ritchie, R.O. Grain-boundary engineering markedly reduces susceptibility to intergranular hydrogen embrittlement in metallic materials. *Acta Mater.* **2009**, *57*, 4148–4157. [[CrossRef](#)]
23. Eliaz, N.; Shachar, A.; Tal, B.; Eliezer, D. Characteristics of hydrogen embrittlement, stress corrosion cracking and tempered martensite embrittlement in high-strength steels. *Eng. Fail. Anal.* **2002**, *9*, 167–184. [[CrossRef](#)]

Disclaimer/Publisher’s Note: The statements, opinions and data contained in all publications are solely those of the individual author(s) and contributor(s) and not of MDPI and/or the editor(s). MDPI and/or the editor(s) disclaim responsibility for any injury to people or property resulting from any ideas, methods, instructions or products referred to in the content.